Functional SNP in the microRNA-367 binding site in the 3′UTR of the calcium channel ryanodine receptor gene 3 (*RYR3*) affects breast cancer risk and calcification

Lina Zhang[a,b,c], Yuexin Liu[c], Fengju Song[a,b], Hong Zheng[a,b], Limei Hu[c], Hong Lu[b,d], Peifang Liu[b,d], Xishan Hao[a,b,d], Wei Zhang[c,1], and Kexin Chen[a,b,1]

Departments of [a]Epidemiology and Biostatistics and [d]Radiology, Tianjin Medical University Cancer Hospital and Institute, Tianjin 300060, People's Republic of China; [b]Key Laboratory of Breast Cancer Prevention and Therapy, Tianjin Medical University, Ministry of Education, Tianjin 300060, People's Republic of China; and [c]Department of Pathology, University of Texas M. D. Anderson Cancer Center, Houston, TX 77030

Edited by Webster K. Cavenee, Ludwig Institute, University of California at San Diego, La Jolla, CA, and approved July 11, 2011 (received for review March 01, 2011)

We have evaluated and provided evidence that the ryanodine receptor 3 gene (*RYR3*), which encodes a large protein that forms a calcium channel, is important for the growth, morphology, and migration of breast cancer cells. A putative binding site for microRNA-367 (miR-367) exists in the 3′UTR of *RYR3*, and a genetic variant, rs1044129 A→G, is present in this binding region. We confirmed that miR-367 regulates the expression of a reporter gene driven by the *RYR3* 3′UTR and that the regulation was affected by the *RYR3* genotype. A thermodynamic model based on base pairing and the secondary structure of the *RYR3* mRNA and miR-367 miRNA showed that miR-367 had a higher binding affinity for the A genotype than for the G genotype. The rs1044129 SNP was genotyped in 1,532 breast cancer cases and 1,600 healthy Chinese women. The results showed that compared with the AA genotype, G was a risk genotype for breast cancer development and was also associated with breast cancer calcification and poor survival. Thus, rs1044129 is a unique SNP that resides in a miRNA-gene regulatory loop that affects breast cancer risk, calcification, and survival.

Ryanodine receptor 3 (RYR3), the third isoform of the RYR family, is a Ca^{2+}-induced Ca^{2+} release (CICR) channel protein located in the sarcoplasmic reticulum that plays a key role in controlling cytosolic calcium levels (1, 2). RYRs are commonly expressed in breast cancer, and there is a correlation between RYR levels and tumor grade (3). The stratification of patients with breast cancer into clinically relevant subtypes is an essential step toward personalized medicine. Several biomarkers contributing to breast cancer prognosis have been identified in the form of oncogenic mutations (4, 5) or genetic polymorphisms, such as SNPs (6, 7). Tissue calcification commonly occurs in the breast and is a risk and prognosis factor for breast cancer (8, 9). Because of its central role in calcium homeostasis, it is conceivable that RYR3 plays a role in breast calcification. Calcium channels are important for calcium homeostasis, which is associated with physiological and pathophysiological processes of the mammary gland, and may represent potential drug targets for the treatment of breast cancer (10–12).

MicroRNAs (miRNAs) are evolutionarily conserved, endogenous, single-stranded, noncoding RNA molecules that are reported to be involved in many biological processes, including cell proliferation, apoptosis, and tumorigenesis, through their regulation of gene expression (13). Most miRNAs bind to target sequences located within the 3′-untranslated region (3′UTR) of mRNAs by base pairing, resulting in the cleavage of target mRNAs or repression of their translation (14). SNPs are the most frequent variation in the human genome, and they occur once every several hundred base pairs throughout the genome. An increasing number of 3′UTR SNPs located in miRNA binding sites have been reported to be associated with cancers (15–17) and drug response (18), presumably because of the differential binding affinities of the SNPs for miRNA. Polymorphisms in these miRNA binding sites in the 3′UTRs of target genes represent a group of genetic variations that modulate the regulatory loop between miRNAs and their target genes (18, 19). Sequence-based bioinformatic predictions have identified a number of these types of SNPs, which has provided candidates for experimental verifications and case-control studies to determine their importance (20). Recently, the SNP rs1044129A→G in the 3′UTR of the *RYR3* gene was reported through a genome-wide analysis of EST databases associated with cancer risk susceptibility (21). However, it is unclear if this SNP is functional and whether it is associated with breast cancer risk and prognosis.

In this study, we first provide evidence that the *RYR3* gene is an important regulator of breast cancer cell growth, morphology, and migration. We then functionally validate SNP rs1044129, which is located in the miR-367 binding site in the 3′UTR of *RYR3*. Finally, we used a case-control study to demonstrate that the SNP rs1044129 is an important genetic variant for breast cancer risk and poor survival.

Results

Modulation of RYR3 Affects Cell Proliferation, Morphology, Migration, and Intracellular Calcium Influx. The function of RYR3 has been difficult to study because of its large molecular mass (550 kDa). To demonstrate that RYR3 functions in breast cancer cells, we took a loss-of-function approach by treating two breast cancer cell lines (MCF-7 and MDA-MB-231) with RYR3 siRNA to decrease its expression. Real-time PCR assay and immunofluorescence staining analyses showed that RYR3 siRNA down-regulated the endogenous RYR3 mRNA and protein levels (Fig. 1 *A* and *B*). We next evaluated the growth, morphology, and migration of the siRNA-treated cells, as well as the calcium influx. Our results showed that knockdown of RYR3 significantly inhibited the growth and migration of both breast cancer cell lines examined (Fig. 1 *C* and *D*) and increased the intracellular calcium level (Fig. 1*E*). Consistent with calcium being an important regulator of cell-cell adhesion, we observed a noticeable change in the morphology of RYR3 siRNA-treated cells, which was easily visualized after staining for F-actin with phalloidin and an E-cadherin antibody (Fig. 1*F*).

SNP rs1044129 A→G Within the miR-367 Binding Site in the *RYR3* 3′UTR Is a Functional Regulatory Site. Using both TargetScan (version 5.1; http://www.targetscan.org) and the miRNA Web server miRBase (http://www.mirbase.org) (22), we determined that the *RYR3* 3′UTR harbors a putative miR-367 miRNA

Author contributions: F.S., W.Z., and K.C. designed research; L.Z., H.Z., L.H., H.L., P.L., X.H., W.Z., and K.C. performed research; L.H. and P.L. contributed new reagents/analytic tools; L.Z., Y.L., and H.L. analyzed data; and L.Z., Y.L., W.Z., and K.C. wrote the paper.

The authors declare no conflict of interest.

This article is a PNAS Direct Submission.

[1]To whom correspondence may be addressed. E-mail: wzhang@mdanderson.org or chenkexin1963@yahoo.com.

This article contains supporting information online at www.pnas.org/lookup/suppl/doi:10.1073/pnas.1103360108/-/DCSupplemental.

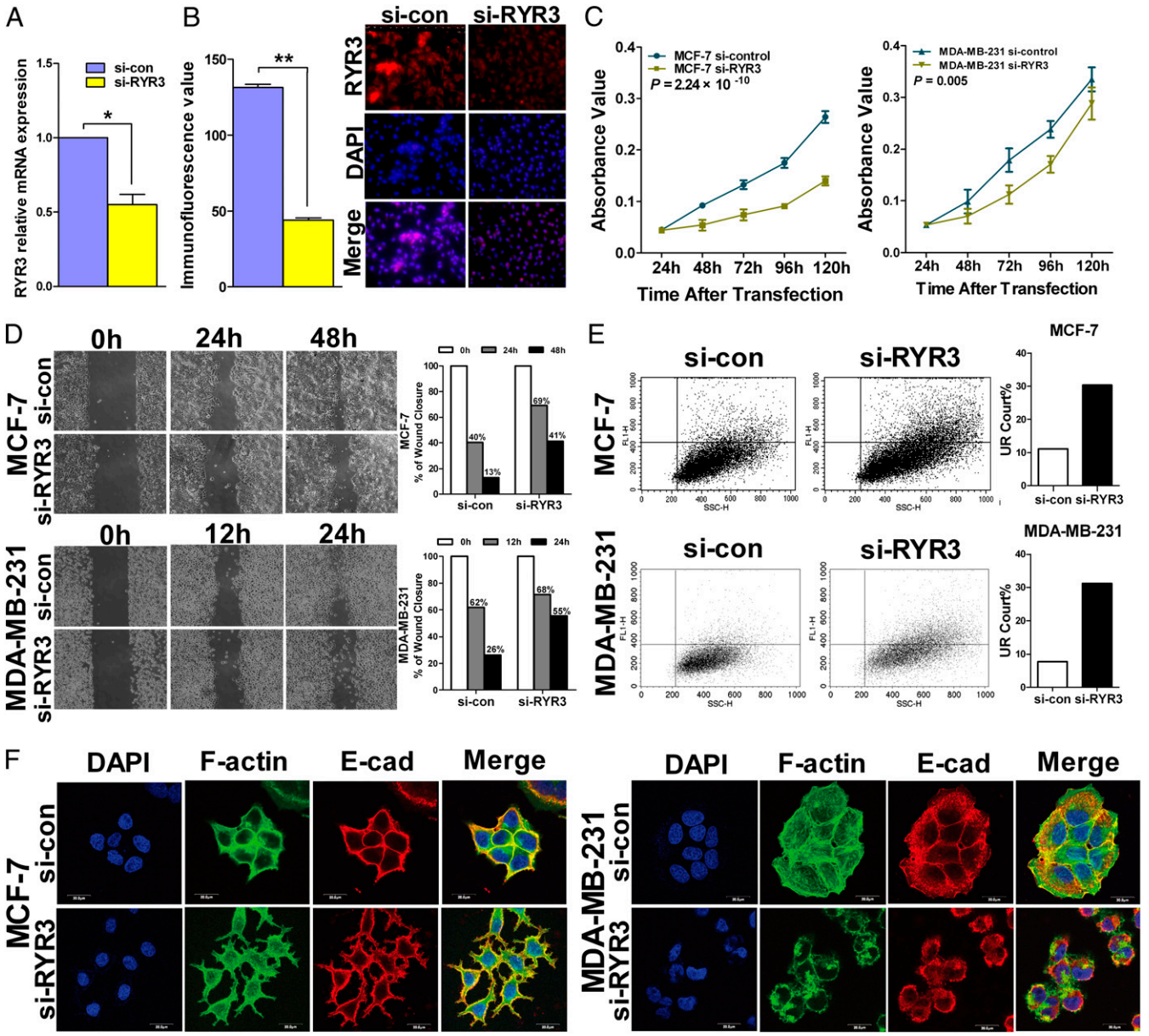

Fig. 1. Role of RYR3 in breast cancer cell growth, migration, and morphology as well as intracellular calcium level. (*A*) After transfection of small interfering (si)-RYR3 for 16 h, RYR3 mRNA expression was measured by real-time quantitative PCR and shown to be down-regulated (*$P = 0.0002$). (*B*) After transfection of si-RYR3 for 48 h, RYR3 protein expression was examined by immunofluorescence and found to be down-regulated (**$P = 0.023$). (*C*) MTT assay showing cell growth viability. The RYR3 knockdown groups (yellow) significantly inhibit cell growth in comparison to si-control cell groups (blue). (*D*) Area of wound coverage was calculated by Cellprofiler software (www.cellprofiler.org) and normalized to the area of the zero time point. (*E*) Determination of the intracellular calcium levels using Fluo-4 AM staining and flow cytometry. Comparison of Fluo-4 AM loading in breast cancer cells transfected with si-control and si-RYR3. The percentages displayed represent the number of cells with calcium, measured by fluorescence in FL1 (green fluorescence signal received by the photomultiplier tube). The percentage of cells in the upper right quadrant (cells single-stained with Fluo-4 AM) represents the relative calcium concentration. FL1; UR, upper right. (*F*) Cells were fixed and stained with phalloidin to detect F-actin (green) and an E-cadherin antibody (red). DAPI was used to stain the nuclei (blue). The images were taken by confocal microscopy. There was an apparent near loss of cell membrane-bound E-cadherin in the si-RYR3–treated cells. (Scale bar, 20 μm.)

binding site (Fig. 2*A*). A nucleotide at position rs1044129 located 13 bp upstream of the miRNA seed binding site is conserved in mice and humans (UCSC Genome Browser; http://genome.ucsc.edu/). In addition, a SNP at the rs1044129A site (rs1044129 A→G) was reported with a minor allele frequency of about 0.45 in the cancer population (21). In this paper, we refer to the A genotype as WT and the G genotype as mutant unless otherwise specified.

Because this SNP (rs1044129) is located near the miRNA-367 binding site, we hypothesized that the SNP would lead to differential regulation of *RYR3* by miR-367 owing to the differential binding affinity of miR-367 for the two *RYR3* 3′UTR genotypes. First, we used a thermodynamic model (Fig. 2*B*) to calculate the different energy terms, and we then constructed the corresponding binding energy diagrams for each genotype (Fig. 2 *C* and *D*). The higher energy of the dissociated target, E_{target}, and smaller activation energy, $\Delta E_{(a)}$, of the A genotype indicated that this genotype was more accessible for miR-367 than the G genotype ($\Delta E_{(a)}'$) variant. Furthermore, the binding energy, $\Delta E_{(b)}$ (equivalent to the interaction score $\Delta\Delta G$) (23), of the A

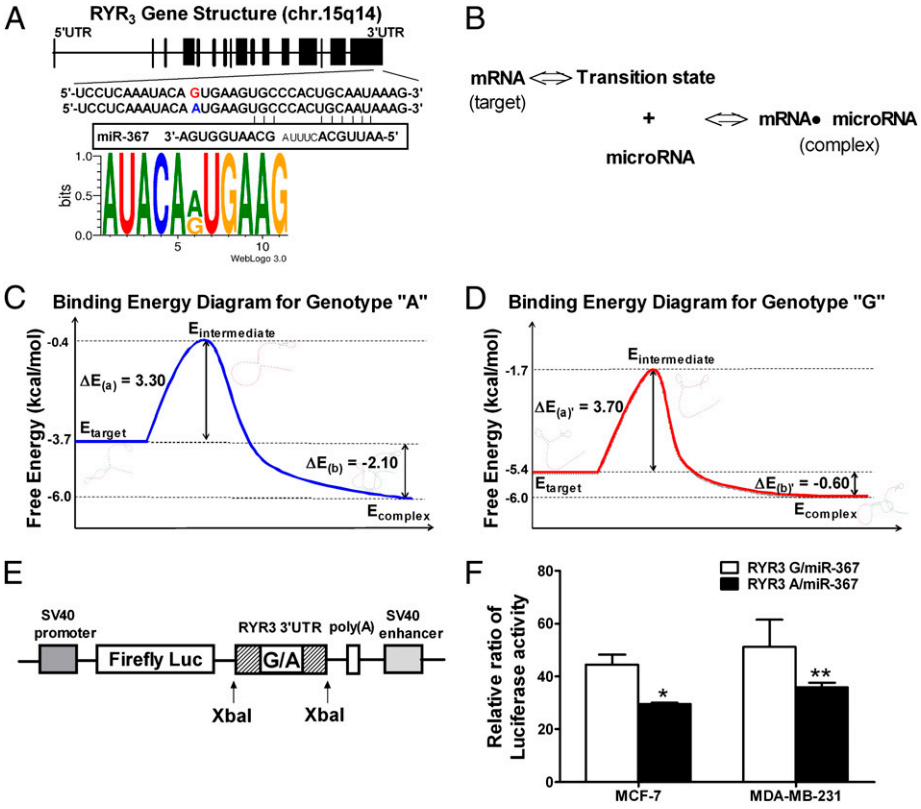

Fig. 2. Functional validation of the miR-367 binding site in the RYR3 3′UTR and the influence of the SNP rs1044129. (*A*) RYR3 gene structure and A/G polymorphism in the *RYR3* 3′UTR at the miR-367 binding site. chr., chromosome. (*B*) Illustration of miRNA-target binding process in which the target is first transitioned to the intermediate state by unpairing the seed target nucleotides and then forms the miRNA-bound mRNA complex when binding with the miRNA. (*C* and *D*) Secondary structure-based energies at different stages of the binding process, where the activation energy, $\Delta E_{(a)}$, is the energy difference between the transition state and the original target and the binding energy, $\Delta E_{(b)}$, is the energy difference between the complex and target. A schematic of the binding energy diagram for the A variant (*C*) and the G variant (*D*) is shown. (*E*) *RYR3* 3′UTR was cloned into the PGL3 control plasmid at the XbaI enzyme site. (*F*) Twenty-four hours after transfection of the reporter gene and miR-367 mimic, the A allele construct had significantly less relative luciferase activity than the reporter bearing the G allele in both MCF-7 (*P = 0.025) and MDA-MB-231 (**P = 0.044) cell lines.

genotype [$\Delta E_{(b)}$ = −2.10 kcal/mol] was almost 3.5-fold smaller than that of the G genotype [$\Delta E_{(b)}{}'$ = −0.6 kcal/mol], suggesting that miR-367 has a higher binding affinity for the A genotype (Fig. S1 *A*–*C*).

We next performed a reporter gene assay to validate the computational prediction and to test the hypothesis that miR-367 more robustly regulates the A allele. We cloned the *RYR3* 3′UTR fragments with either the G or A allele into a luciferase reporter vector (Fig. 2*E*). Reporter gene vectors containing either the G or A allele and the miR-367 mimic (or control) were transiently transfected into MCF-7 and MDA-MB-231 cell lines, and the relative Firefly luciferase to *Renilla* luciferase activity was measured. Consistent with our computational modeling prediction, we found that the miR-367 mimic reduced the luciferase reporter gene activity more significantly when it was regulated by the A allele variant of the *RYR3* 3′UTR in both the MCF-7 (P = 0.025) and MDA-MB-231 (P = 0.044; Fig. 2*F*) cell lines.

To validate whether miR-367 regulates the expression of the endogenous RYR3, miR-367 mimic or inhibitor was transfected into MDA-MB-231 breast cancer cells. Real-time PCR assay and immunofluorescence staining analyses showed that miR-367 mimic down-regulated the endogenous RYR3 mRNA and protein levels (Fig. 3 *A*–*C*). Consistent with siRNA knockdown results, transfection of miR-367 mimic led to inhibition of growth and migration as well as change of cell morphology to a more rounded shape with weakened cell-cell contacts (Fig. S2).

G Genotype Increases Breast Cancer Risk and Calcification. To determine the potential role of the RYR3 3′UTR SNP (rs1044129) in breast cancer further, we used a population-based approach to evaluate the effect of the SNP rs1044129 on breast cancer risk and prognosis. We performed a case-control study that included 1,532 breast cancer cases and 1,600 healthy controls. Genotype frequencies among the controls did not show significant departures from Hardy–Weinberg equilibrium (P = 0.535). As shown in Table S1, the average age at diagnosis for the cases was 52.03 ± 10.75 y, which was similar to that for the controls at recruitment (51.91 ± 10.62 y; P = 0.740). In the unconditional logistic regression analysis of the genotypes, we found that compared with the AA genotype carriers, patients with the G (GG + GA) allele genotypes had a statistically significantly higher risk for cancer [adjusted odds ratio (aOR) = 1.26, 95% confidence interval (CI): 1.03–1.54; P = 0.028], especially postmenopausal women (aOR = 1.31; 95% CI: 1.00–1.72; Table S2). Additional stratified analyses of the associations between breast cancer and hormonal risk factors by *RYR3* genotype are presented in Fig. 4. There was a stronger association between the *RYR3* G allele genotypes and cancer risk than for the AA genotype.

We next preformed a case-only analysis to examine the association between the rs1044129 genotypes and clinical and pathological features. Breast calcification, as seen on mammograms, is an important diagnostic marker for breast cancer and is possibly a result of dysregulation of calcium metabolism. To evaluate whether the rs1044129 polymorphism in the 3′UTR of the calcium receptor gene *RYR3* is related to calcification, we reviewed the available mammograms of 1,424 breast cancer cases and stratified these cases into two groups: those positive or negative for microcalcification. We found that compared with the AA genotype, the GA + GG genotypes were associated with microcalcification-positive breast cancers [odds ratio (OR) = 1.52; 95% CI: 1.21–1.90; $P = 2.66 \times 10^{-4}$; Table S3].

To evaluate whether the rs1044129 polymorphism was associated with RYR3 expression in breast cancer, we examined RYR3 protein expression in tumor tissues by immunohistochemistry in 60 patients with breast cancer. The results showed that tumors have higher expression of RYR3 in GG and GA genotypes (Fig. 5 *A*–*J*). We also measured the miR-367 levels in the same tumor tissues, and the results showed there were no significant differences between the three genotype groups (Fig. 5*K*).

We subsequently determined whether the rs1044129 genotypes and the associated microcalcification phenotypes could be used to predict patient survival. We selected 1,125 cases that had been followed up for at least 24 mo (the median follow-up time for this cohort was 32 mo). We then analyzed the correlation of

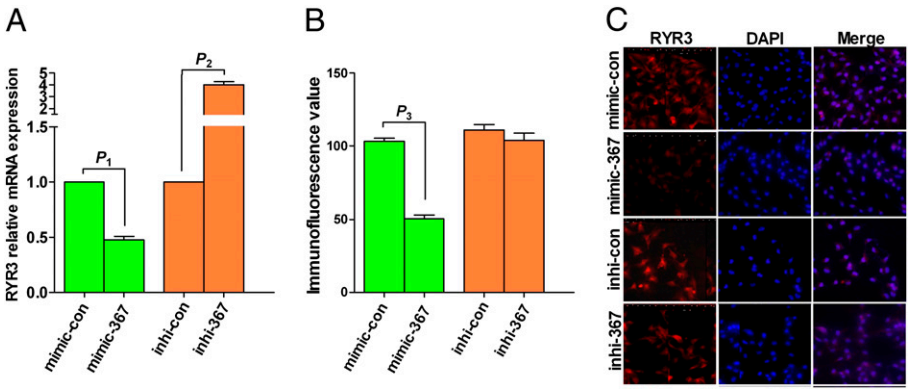

Fig. 3. Endogenous RYR3 mRNA and protein expression in MDA-MB-231 cells after transfection of the miR-367 mimic. (*A*) After transfection of miR-367 mimic (mimic-367) for 16 h, RYR3 mRNA expression was measured by real-time quantitative PCR and shown to be down-regulated, similar to the effect of small-interfering (si)-RYR3 ($P_1 = 0.002$). In contrast, the RYR3 mRNA level was increased in cells transfected with miR-367 inhibitor (inhi-367) ($P_2 = 0.004$). (*B*) After transfection of miR-367 mimic or si-RYR3 for 48 h, RYR3 protein expression was examined by immunofluorescence and found to be down-regulated ($P_3 = 1.89 \times 10^{-7}$). The level of RYR3 staining was not further elevated in cells transfected with miR-367 inhibitor. (*C*) Cells were fixed by 4% paraformaldehyde (0.4 g paraformaldehyde/100 ml PBS) and then stained with the anti-RYR3 antibody at a dilution of 1:500. Fluorescence-labeled secondary antibody was used to show RYR3 (red), and DAPI staining was used to stain the nuclei (blue).

the rs1044124 genotypes or microcalcification with overall survival (OS) and progression-free survival (PFS). Kaplan–Meier survival curves showed there was no association between different genotypes or calcification features and OS (Fig. 6 *A* and *C*). However, compared with the AA genotype, the G allele genotypes and microcalcification were significantly associated with poor PFS (Fig. 6 *B* and *D*). The univariate Cox regression analysis of the correlation between PFS and genotype or calcification is shown in Table S4.

Discussion

In this study, we determined that the G allele of rs1044129 was associated with breast cancer risk, calcification, and PFS, suggesting that this genetic variant is important for both cancer initiation and cancer progression. Furthermore, we characterized rs1044129 as a unique SNP that confers a genetic effect (sequence variation) on gene regulation by an epigenetic factor (miR binding). Specifically, miR-367 binds more tightly to the A allele of rs1044129 and represses RYR3 expression more strongly than to the G allele.

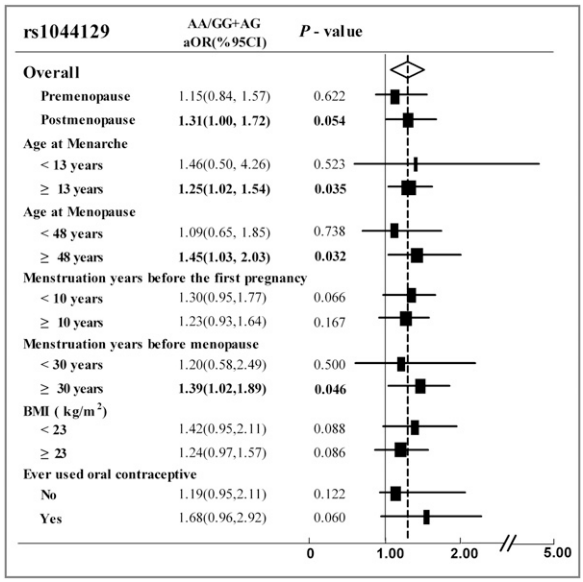

Fig. 4. Forest plot of the association between the RYR3 rs1044129 genotypes and breast cancer risk.

Polymorphisms in the 3′UTRs of several genes have been reported to be associated with diseases by affecting miRNA-regulated gene/protein expression (24). Different from previously reported examples, where the SNPs are located in the seed binding regions of the miR, rs1044129 is located outside the seed binding region. Using computational modeling, we found that the G and A variants assume different secondary structures and the thermodynamics clearly favor the binding of miR-367 to the A form. We performed a number of wet-laboratory experiments using reporter gene assays and validated that miR-367 indeed targets the predicted region in the *RYR3* 3′UTR and that miR-367 represses the A allele more than the G allele. Thus, this population-based study, coupled with functional validation, revealed an important genetic risk factor for breast cancer, which is mediated by differential regulation of *RYR3* by miR-367.

It has been established that decreased calcium and vitamin D intake is associated with carcinogenesis of the mammary gland (25, 26). In addition, breast calcification is an important risk factor for breast cancer (8, 27). RYR3 is a CICR protein that plays an important role in cellular Ca^{2+} homeostasis (28). Our case-control study suggests that the *RYR3* gene is critical to the development of breast cancer, possibly by regulating calcium metabolism in breast tissues. Our results showed that the *RYR3* G allele genotypes (GG + GA) increased the risk for breast cancer in Chinese women, especially postmenopausal women. It is likely that the *RYR3* A→G polymorphism may regulate the intracellular Ca^{2+} concentration and increase susceptibility to breast cancer. The increased risk associated with this genetic variant in postmenopausal women is consistent with the knowledge that estrogens are regulators of calcium influx (29) and that postmenopausal women absorb calcium less efficiently (30, 31). It has been postulated that microcalcification is a result of abnormal calcium deposition and mineralization of necrotic debris (32, 33). We found that the *RYR3* G allele (GG + GA) genotypes were significantly associated with microcalcification in breast cancer tissues. Thus, our study may have identified a key regulatory gene that is critical in the physiological process of breast cancer microcalcification and is a potential target for intervention.

In summary, rs1044129 modulates the epigenetic regulation of a key calcium metabolism gene, *RYR3*, through miR-367. In addition, this study has uncovered the rs1044129 polymorphism as playing an important role in breast cancer susceptibility and prognosis. Thus, further investigation of this regulatory network is warranted.

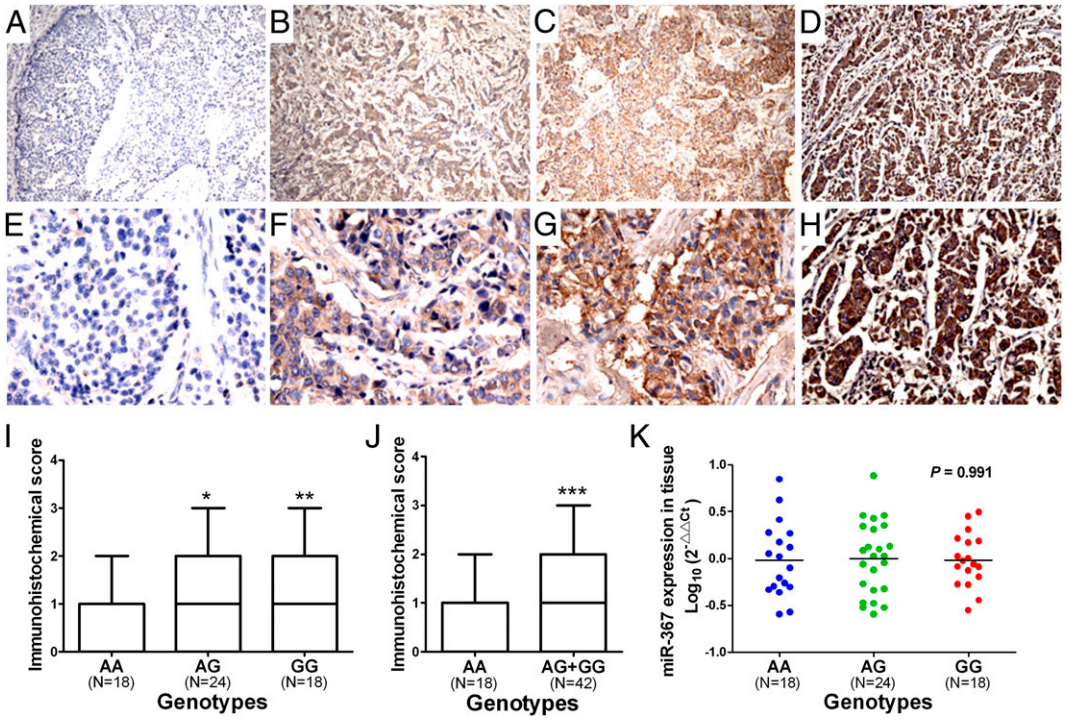

Fig. 5. Correlation of RYR3 expression with genotype in breast tumor tissues. Examples of different degrees of staining in tissue sections: – (*A*), + (*B*), ++ (*C*), and +++ (*D*). (*E–H*) Higher magnification images of *A–D*, respectively. (Magnification: *A–D*, 100×; *E–H*, 400×). (*I*) Semiquantitative levels of immunohistochemical staining in samples with AA, AG, or GG genotypes. AG and GG genotypes have a higher level of RYR3 than the AA genotype. **P* = 0.047; ***P* = 0.048. (*J*) Compared with the AA genotype, G (GG + GA) genotypes have a higher level of RYR3 in immunohistochemistry. ****P* = 0.024. (*K*) Levels of miR-367 in breast cancer tissues of three genotypes are similar.

Materials and Methods

Cell Growth and Migration, Intracellular Calcium Levels, and Changes in Cell Morphology. The human breast cancer cell lines MCF-7 and MDA-MB-231 were obtained from the American Type Culture Collection. Cell proliferation was determined by the 3-[4, 5-dimethylthiazol-2-yl]-2, 5-dephenyl tetrazolium bromide (MTT) method (34). Cell migration was analyzed by a wound healing assay (35). The intracellular free calcium level was measured by flow cytometry by using Fluo-4 AM as described previously (36). CellQuest software (BD Bioscience) was used for fluorescence analysis. The cell morphology images were captured by confocal microscopy. More detailed information regarding cell culture, MTT, and RNA isolation can be found in *SI Text*.

Real-Time Quantitative PCR Assay. RYR3 mRNA and miR-367 expression was quantified using TaqMan miRNA assays (Applied Biosystems) with modifications as described in detail in *SI Text*.

Immunofluorescence Staining. The process of rabbit anti-RYR3 (Millipore) or mouse anti–E-cadherin (BD Biosciences) immunofluorescence staining is described in *SI Text*.

Thermodynamic Model for the miRNA-Target Interaction. Targetscan 5.1 (http://www.targetscan.org) and Miranda (http://www.microrna.org) were used to identify miR-367 as being likely to bind to the rs1044129 region. To investigate the binding affinity of miR-367 for the rs1044129 region with

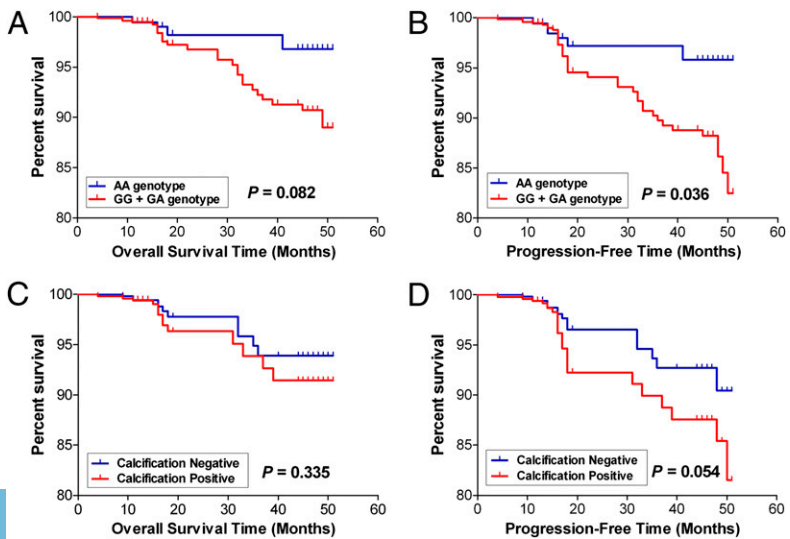

Fig. 6. Association of the *RYR3* 3′UTR SNP or calcification with survival. Kaplan–Meier breast cancer-specific survival curves of OS (*A*) and PFS (*B*) of patients with the GG + GA phenotypes vs. the AA genotype and OS (*C*) and PFS (*D*) of patients with calcification-positive breast cancer vs. calcification-negative breast cancer. *P* values are from the log-rank test.

different genotypes (A and G in this case), we assessed the secondary structure-based energies of molecules involved in the binding process using a parameter-free thermodynamic model (37, 38). A 3′-supplementary binding site of miR-367 centering on miRNA nucleotides 13–15 exists and was incorporated in this computation along with the seed binding site (Fig. S3*A*). The other marginal 6-mer binding sites located at the coding region of RYR3 (Fig. S3*A*) have significantly reduced binding capacity compared with the 3′UTR 7-mer-A1 target site [seed binding region followed by an A nucleotide, which has been shown to have a more favorable binding energy (39)], and therefore were not included in this computation. The details are described in *SI Text*.

Luciferase Reporter Gene Assay. The details are described in *SI Text*.

Subjects. The case-control study included 1,538 patients with breast cancer and 1,605 healthy female controls. We obtained 1,424 cases with mammogram information, which were reviewed and categorized according to the Breast Imaging Reporting and Data System by two radiologists (40, 41). The study protocol was approved by the Institutional Review Board (IRB) at the TCIH. All participants gave informed consent to use their samples for research purposes. The details are described in *SI Text*.

Genotyping. Genomic DNA was extracted from peripheral blood samples as previously described (42). We genotyped the A/G SNP in the 3′UTR of *RYR3* (rs1044129) using the TaqMan allelic discrimination method (Applied Biosystems). The details are described in *SI Text*.

Immunohistochemical Methods. Immunohistochemistry was essentially done as described (43). Formalin-fixed and paraffin-embedded blocks of the 60 breast cancer specimens were analyzed using a rabbit anti-RYR3 antibody (AB9082; Millipore) at a dilution of 1:500. Stained tissue sections were evaluated by two expert pathologists, and the details are described in *SI Text*.

Statistical Analysis. The details are described in *SI Text*.

ACKNOWLEDGMENTS. We thank Yingmei Wang and Hanyin Cheng of the Department of Pathology at the University of Texas M. D. Anderson Cancer Center for her technical assistance; Jifang Wang, Yanrui Zhao, Hongwei Han, Yan Guo, and Lei Lei of the Tianjin Medical University Cancer Institute and Hospital for assistance in collecting clinical information and their technical assistance; and Kate J. Newberry of the Department of Scientific Publications at the University of Texas M. D. Anderson Cancer Center for editing this manuscript. This work was supported partially by the National Natural Science Foundation of China (Grants 30872172 and 30771844), program for Changjiang Scholars and Innovative Research Team in University in China (Grant IRT1076), National Key Scientific and Technological Project (Grant 2011ZX09307-001-04), Tianjin Science and Technology Committee Foundation (Grants 08ZCGHZ02000, 08JCZDJC23600, 09ZCZDSF04800, and 09ZCZDSF04700), and Major State Basic Research Development Program of China (973 Program, Grant 2009CB918903). The tissue bank is jointly supported by the Tianjin Medical University Cancer Institute and Hospital and the US National Foundation for Cancer Research. This research was also supported in part by the National Institutes of Health through M. D. Anderson Cancer Center Support Grant CA016672.

1. Giannini G, Clementi E, Ceci R, Marziali G, Sorrentino V (1992) Expression of a ryanodine receptor-Ca2+ channel that is regulated by TGF-beta. *Science* 257:91–94.
2. Bennett DL, et al. (1996) Expression and function of ryanodine receptors in non-excitable cells. *J Biol Chem* 271:6356–6362.
3. Abdul M, Ramlal S, Hoosein N (2008) Ryanodine receptor expression correlates with tumor grade in breast cancer. *Pathol Oncol Res* 14:157–160.
4. Miki Y, et al. (1994) A strong candidate for the breast and ovarian cancer susceptibility gene BRCA1. *Science* 266:66–71.
5. Wooster R, et al. (1994) Localization of a breast cancer susceptibility gene, BRCA2, to chromosome 13q12-13. *Science* 265:2088–2090.
6. Varadi V, et al. (2009) Polymorphisms in telomere-associated genes, breast cancer susceptibility and prognosis. *Eur J Cancer* 45:3008–3016.
7. Yu JC, et al. (2009) Genetic susceptibility to the development and progression of breast cancer associated with polymorphism of cell cycle and ubiquitin ligase genes. *Carcinogenesis* 30:1562–1570.
8. Thomas DB, et al. (1993) Mammographic calcifications and risk of subsequent breast cancer. *J Natl Cancer Inst* 85:230–235.
9. Thurfjell E, Thurfjell MG, Lindgren A (2001) Mammographic finding as predictor of survival in 1-9 mm invasive breast cancers. Worse prognosis for cases presenting as calcifications alone. *Breast Cancer Res Treat* 67:177–180.
10. Montell C (2005) The latest waves in calcium signaling. *Cell* 122:157–163.
11. Hakimuddin F, Paliyath G, Meckling K (2006) Treatment of mcf-7 breast cancer cells with a red grape wine polyphenol fraction results in disruption of calcium homeostasis and cell cycle arrest causing selective cytotoxicity. *J Agric Food Chem* 54: 7912–7923.
12. Baldi C, Vazquez G, Boland R (2003) Capacitative calcium influx in human epithelial breast cancer and non-tumorigenic cells occurs through Ca2+ entry pathways with different permeabilities to divalent cations. *J Cell Biochem* 88:1265–1272.
13. Ambros V (2004) The functions of animal microRNAs. *Nature* 431:350–355.
14. Meister G, Tuschl T (2004) Mechanisms of gene silencing by double-stranded RNA. *Nature* 431:343–349.
15. Song FJ, et al. (2009) An miR-502-binding site single-nucleotide polymorphism in the 3′-untranslated region of the SET8 gene is associated with early age of breast cancer onset. *Clin Cancer Res* 15:6292–6300.
16. Ratner E, et al. (2010) A KRAS-variant in ovarian cancer acts as a genetic marker of cancer risk. *Cancer Res* 70:6509–6515.
17. Chin LJ, et al. (2008) A SNP in a let-7 microRNA complementary site in the KRAS 3′ untranslated region increases non-small cell lung cancer risk. *Cancer Res* 68: 8535–8540.
18. Mishra PJ, et al. (2007) A miR-24 microRNA binding-site polymorphism in dihydrofolate reductase gene leads to methotrexate resistance. *Proc Natl Acad Sci USA* 104:13513–13518.
19. Morley M, et al. (2004) Genetic analysis of genome-wide variation in human gene expression. *Nature* 430:743–747.
20. Chen K, et al. (2008) Polymorphisms in microRNA targets: A gold mine for molecular epidemiology. *Carcinogenesis* 29:1306–1311.
21. Yu ZB, et al. (2007) Aberrant allele frequencies of the SNPs located in microRNA target sites are potentially associated with human cancers. *Nucleic Acids Res* 35: 4535–4541.
22. Griffiths-Jones S, Saini HK, van Dongen S, Enright AJ (2008) miRBase: Tools for microRNA genomics. *Nucleic Acids Res* 36(Database issue):D154–D158.
23. Kertesz M, Iovino N, Unnerstall U, Gaul U, Segal E (2007) The role of site accessibility in microRNA target recognition. *Nat Genet* 39:1278–1284.
24. Nicoloso MS, et al. (2010) Single-nucleotide polymorphisms inside microRNA target sites influence tumor susceptibility. *Cancer Res* 70:2789–2798.
25. Xue L, Lipkin M, Newmark H, Wang J (1999) Influence of dietary calcium and vitamin D on diet-induced epithelial cell hyperproliferation in mice. *J Natl Cancer Inst* 91: 176–181.
26. Goodwin PJ, Ennis M, Pritchard KI, Koo J, Hood N (2009) Prognostic effects of 25-hydroxyvitamin D levels in early breast cancer. *J Clin Oncol* 27:3757–3763.
27. Tse GM, Tan PH, Cheung HS, Chu WC, Lam WW (2008) Intermediate to highly suspicious calcification in breast lesions: A radio-pathologic correlation. *Breast Cancer Res Treat* 110:1–7.
28. Takeshima H, et al. (1995) Ca(2+)-induced Ca2+ release in myocytes from dyspedic mice lacking the type-1 ryanodine receptor. *EMBO J* 14:2999–3006.
29. Russo J, Mills MJ, Moussalli MJ, Russo IH (1989) fluence of human breast development on the growth properties of primary cultures. *In Vitro Cell Dev Biol* 25:643–649.
30. Heaney RP, Recker RR, Stegman MR, Moy AJ (1989) Calcium absorption in women: Relationships to calcium intake, estrogen status, and age. *J Bone Miner Res* 4: 469–475.
31. Heaney RP, Recker RR, Saville PD (1978) Menopausal changes in calcium balance performance. *J Lab Clin Med* 92:953–963.
32. Millis RR, Davis R, Stacey AJ (1976) The detection and significance of calcifications in the breast: A radiological and pathological study. *Br J Radiol* 49:12–26.
33. Castellanos MR, et al. (2008) Breast cancer screening in women with chronic kidney disease: The unrecognized effects of metastatic soft-tissue calcification. *Nat Clin Pract Nephrol* 4:337–341.
34. Kanematsu S, et al. (2010) Autophagy inhibition enhances sulforaphane-induced apoptosis in human breast cancer cells. *Anticancer Res* 30:3381–3390.
35. Morin P, Wickman G, Munro J, Inman GJ, Olson MF (2011) Differing contributions of LIMK and ROCK to TGFβ-induced transcription, motility and invasion. *Eur J Cell Biol* 90:13–25.
36. Réthi B, et al. (2002) Flow cytometry used for the analysis of calcium signaling induced by antigen-specific T-cell activation. *Cytometry* 47:207–216.
37. Wuchty S, Fontana W, Hofacker IL, Schuster P (1999) Complete suboptimal folding of RNA and the stability of secondary structures. *Biopolymers* 49:145–165.
38. Mathews DH, Sabina J, Zuker M, Turner DH (1999) Expanded sequence dependence of thermodynamic parameters improves prediction of RNA secondary structure. *J Mol Biol* 288:911–940.
39. Bartel DP (2009) MicroRNAs: Target recognition and regulatory functions. *Cell* 136: 215–233.
40. Obenauer S, Hermann KP, Grabbe E (2005) Applications and literature review of the BI-RADS classification. *Eur Radiol* 15:1027–1036.
41. Gülsün M, Demirkazik FB, Ariyürek M (2003) Evaluation of breast microcalcifications according to Breast Imaging Reporting and Data System criteria and Le Gal's classification. *Eur J Radiol* 47:227–231.
42. Lahiri DK, Schnabel B (1993) DNA isolation by a rapid method from human blood samples: Effects of MgCl2, EDTA, storage time, and temperature on DNA yield and quality. *Biochem Genet* 31:321–328.
43. Charafe-Jauffret E, et al. (2004) Immunophenotypic analysis of inflammatory breast cancers: Identification of an 'inflammatory signature.' *J Pathol* 202:265–273.